Vortex formation of coherent waves in nonseparable mesoscopic billiards

Y. F. Chen and K. F. Huang
Department of Electrophysics, National Chiao Tung University, Hsinchu, Taiwan
(Received 7 August 2003; published 23 December 2003)

We analytically study the vortex formation associated with the classical periodic orbits in a nonseparable quantum billiard. The influence of vortex formation on the quantum flux in the mesoscopic region is clearly demonstrated. Remarkably, the high-order vortex structures in an equilateral triangle billiard display the triangular, swirl, and *kagomè* vortex lattices. The relationship between various vortex lattices is found to rely on the relative phase factor in the coherent state.

DOI: 10.1103/PhysRevE.68.066207 PACS number(s): 05.45.Mt, 03.65.Ge, 03.65.Vf, 67.40.Vs

In recent years, there has been growing attention to the dependence of the vortex configuration on the geometry of mesoscopic thin superconductors [1–3]. The symmetry-induced formation of vortex patterns is important not only for superconductors but also for symmetrically confined superfluids and Bose-Einstein condensates [4,5], which are typically described within the mean-field approximation [6] by a nonlinear equation. Indeed, quantum vortices can appear in a system described by the linear Schrödinger equation [7] such as two-dimensional (2D) square billiards [8]. A renaissance of interest in the quantum billiard problems comes from the result that the analogous experiments for various classical wave systems such as microwave cavities [9–11] and semiconductor lasers [12] have been demonstrated. The studies in progress focus on the vortex formation in 2D mesoscopic billiards [13,14] because of the exact correspondence between the quantum probability flux and the Poynting vector of 2D microwave cavities [15,16].

On the other hand, the experimental results in the ballistic quantum transport revealed that the quantum states associated with the classical periodic orbits play an important role in the striking phenomena of conductance fluctuations [17]. In this work, we analytically study the vortex formation associated with the classical periodic orbits in a 2D mesoscopic equilateral triangle billiard, which is a classically nonseparable but integral system. It is found that the geometry-induced vortex formation gives rise to a conspicuous dissimilarity between the quantum and classical flux. Remarkably, the swirl, triangular, and *kagomè* vortex lattices can be formed in the high-order coherent states with special phase factors.

The three vertices of an equilateral triangle billiard is assumed to be at (0,0), $(a/2,\sqrt{3}a/2)$, and $(-a/2,\sqrt{3}a/2)$, where a is the side length. The formation of classical periodic orbits can be denoted by three parameter $(p,q,\pm\phi)$, where the parameters p and q are nonnegative integers with the restriction that $p \geqslant q$; the parameter ϕ is in the range of 0 to π. The sign $\pm$ and the parameters p and q correspond to the initial angle of the billiard ball by [18]

$$\tan\theta = (\pm)\frac{p-q}{p+1}\frac{1}{\sqrt{3}}, \tag{1}$$

where the initial angle θ is with respect to the horizontal. Assuming the initial position to be on the y axis, the parameter ϕ can be related to the initial position by

$$y = \left(\frac{1}{p+q}\right)\left(\frac{\phi}{\pi}\right)\frac{\sqrt{3}a}{2}. \tag{2}$$

Some sample orbit families are given in Fig. 1. In terms of the p and q, the path lengths can be written as $L_{p,q} = a\sqrt{3}\sqrt{p^2+pq+q^2}$, except for the isolated orbits such as $(1,1,\pi)$ [18].

The eigenstates in an equilateral triangular quantum billiard have been derived by several groups [19,20]. The wave functions for the two degenerate stationary states can be expressed as

$$\Phi^{(1)}_{m,n}(x,y) = \sqrt{\frac{16}{a^2 3\sqrt{3}}}\left\{\cos\left[(m+n)\frac{2\pi}{3a}x\right]\sin\left[(m-n)\times\frac{2\pi}{\sqrt{3}a}y\right] + \cos\left[(2m-n)\frac{2\pi}{3a}x\right]\sin\left[n\frac{2\pi}{\sqrt{3}a}y\right] - \cos\left[(2n-m)\frac{2\pi}{3a}x\right]\sin\left[m\frac{2\pi}{\sqrt{3}a}y\right]\right\} \tag{3}$$

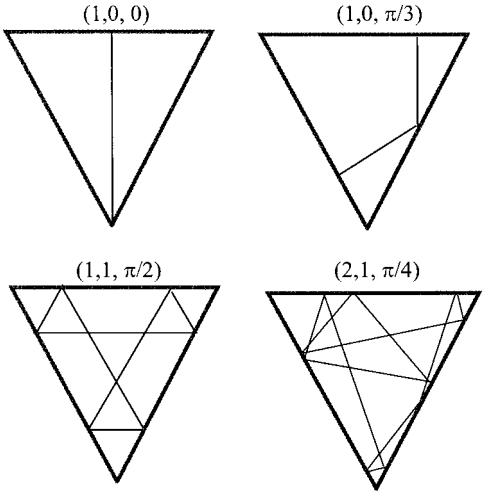

FIG. 1. Some classical periodic orbits (p,q,ϕ) in the equilateral triangle billiard.

and

$$\Phi^{(2)}_{m,n}(x,y)=\sqrt{\frac{16}{a^2 3\sqrt{3}}}\left\{\sin\left[(m+n)\frac{2\pi}{3a}x\right]\sin\left[(m-n)\times\frac{2\pi}{\sqrt{3}a}y\right]-\sin\left[(2m-n)\frac{2\pi}{3a}x\right]\sin\left[n\frac{2\pi}{\sqrt{3}a}y\right]+\sin\left[(2n-m)\frac{2\pi}{3a}x\right]\sin\left[m\frac{2\pi}{\sqrt{3}a}y\right]\right\} \quad (4)$$

for the case of $n>2m$. As it is, the conventional eigenstates do not manifest the properties of classical periodic orbits even in the correspondence limit of large quantum numbers.

For the construction of the coherent states associated with the periodic orbits, it is mandatory to use the traveling wave states from the linear combination of the eigenstates in Eqs. (3) and (4):

$$\Phi_{m,n}(x,y)=\Phi^{(1)}_{m,n}(x,y)+i\Phi^{(2)}_{m,n}(x,y)=\sqrt{\frac{16}{a^2 3\sqrt{3}}}\times\left\{\exp\left[i(m+n)\frac{2\pi}{3a}x\right]\sin\left[(m-n)\frac{2\pi}{\sqrt{3}a}y\right]+\exp\left[-i(2m-n)\frac{2\pi}{3a}x\right]\sin\left[n\frac{2\pi}{\sqrt{3}a}y\right]-\exp\left[-i(2n-m)\frac{2\pi}{3a}x\right]\sin\left[m\frac{2\pi}{\sqrt{3}a}y\right]\right\}. \quad (5)$$

The SU(2) coherent state for the 2D quantum harmonic oscillators has been demonstrated to be well localized on the corresponding classical elliptical trajectory [21]. As in the Schwinger representation of the SU(2) algebra [21] and in terms of $\Phi_{m,n}(x,y)$, the wave functions associated with the periodic orbits $(p,q,\pm\phi)$ in an equilateral triangular quantum billiard are deduced to be

$$\Psi_{N,M}(x,y;p,q,\pm\phi)=\frac{1}{2^{N/2}}\sum_{K=0}^{N}\binom{N}{K}^{1/2}\exp(\pm iK\phi)\times\Phi_{p(K+1),M+q(N-K)}(x,y) \quad (6)$$

with the restriction that $M\geqslant 2p(N+1)$, where the indices M and N indicates the order of the coherent states. Equation (6) indicates that the parameter ϕ is the relative phase between various components of the coherent state. Figure 2 depicts the wave patterns of $|\Psi_{N,M}(x,y;p,q,\phi)|^2$ with $N=20$ and $M=2p(N+1)$ corresponding to the classical trajectories displayed in Fig. 1. On the whole, the distributions of $|\Psi_{N,M}(x,y;p,q,\phi)|^2$ are in good agreement with the classical trajectories. Even so, quantum interference effects not only lead to the wave localization but also result in the interwoven patterns and vortex structures, which cause the quantum flux to be significantly different from the classical picture.

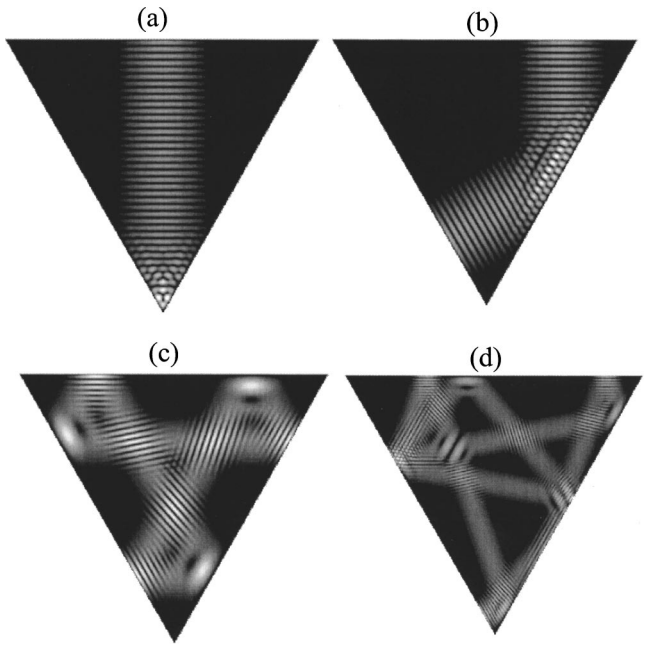

FIG. 2. The wave patterns of $|\Psi_{N,M}(x,y;p,q,\phi)|^2$ from Eq. (6) for $N=20$ and $M=2p(N+1)$ corresponding to the classical trajectories displayed in Fig. 1.

The character of the classical trajectories implied by the coherent states can be manifested by using the identity of $\sin z=(e^{iz}-e^{-iz})/2i$ to rewrite $\Phi_{m,n}(x,y)$ in Eq. (6). Applying the property of the Dirichlet kernel, the maximum intensity of the coherent state in Eq. (6) can be found to localize on the six lines of equation families $qy/\sqrt{3}a\pm(2p+q)x/3a\mp\phi/2\pi=n$, $py/\sqrt{3}a\pm(p+2q)x/3a\pm\phi/2\pi=n$, $(p+q)y/\sqrt{3}a\pm(p-q)x/3a\pm\phi/2\pi=n$ with $n\in Z$, which coincide with the classical trajectories. Therefore, the relative phase factor between various parts of the coherent state has a causal relationship with the localization on the classical trajectories. Note that the quantum flux for the complex conjugate of the coherent state $\Psi^{*}_{N,M}(x,y;p,q,\phi)$ changes to the opposite direction. Therefore, the coherent states, $\Psi_{N,M}\pm i\Psi^{*}_{N,M}$, turn out to be the standing waves.

Strictly speaking, the coherent states in Eq. (6) are not stationary states because the eigenstate components are not exactly degenerate for the Hamiltonian H. Nevertheless, the asymptotic behavior that $\Delta H/\langle H\rangle\to 0$ as $N\to\infty$ ensures the coherent states in Eq. (6) to be stationary states in the classical limit, where $\langle H\rangle$ is the expectation value of the Hamiltonian and ΔH is the dispersion in energy by computing $\sqrt{\langle H^2\rangle-\langle H\rangle^2}$. On the other hand, experimental results [11,12,17] have revealed that the coherent state obtained as a superposition of a few nearly degenerate eigenstates provides a more physical description of a phenomenon than the true eigenstates in the mesoscopic region.

With the coherent state, the probability current density $\vec{J}\propto\mathrm{Im}(\Psi^{*}\nabla\Psi)$ can be calculated to gain physical aspects of the quantum vortices. In separable rectangular billiards [8],

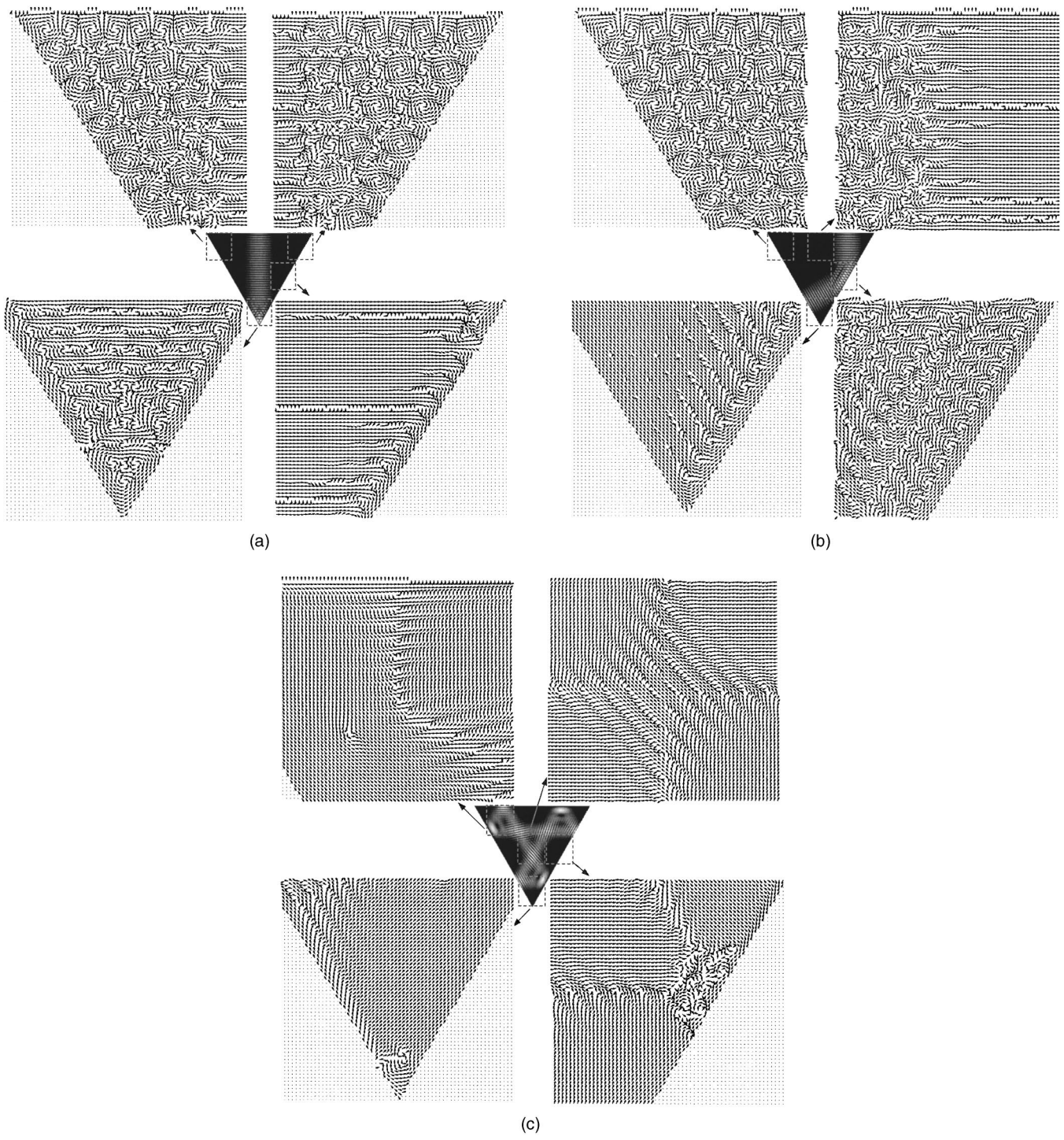

FIG. 3. (a) The normalized quantum flux $\vec{J}/|\vec{J}|$ for several small regions of the coherent states shown in Fig. 2(a). (b) The normalized quantum flux $\vec{J}/|\vec{J}|$ for several small regions of the coherent states shown in Fig. 2(b). (c) The normalized quantum flux $\vec{J}/|\vec{J}|$ for several small regions of the coherent states shown in Fig. 2(c).

the tangents to the quantum streamlines generally coincide with the directions of the classical velocities; the vortex structures form a regular square lattice. In a nonseparable billiard, however, the formation of complex vortex structures gives rise to a conspicuous inconsistency between the quantum flux and the classical velocity fields, as shown in Figs. 3(a)–3(c) for the wave functions displayed in Fig. 2. To show the fine details, Figs. 3(a)–3(c) depict the normalized quantum flux $\vec{J}/|\vec{J}|$ for several small regions. Despite the well localization of the quantum probability on the classical trajectories, the quantum probability flows significantly differ from the classical velocity fields. In particular, the interference-induced quantum vortices play an important role not only in the localization part but also in the low probabil-

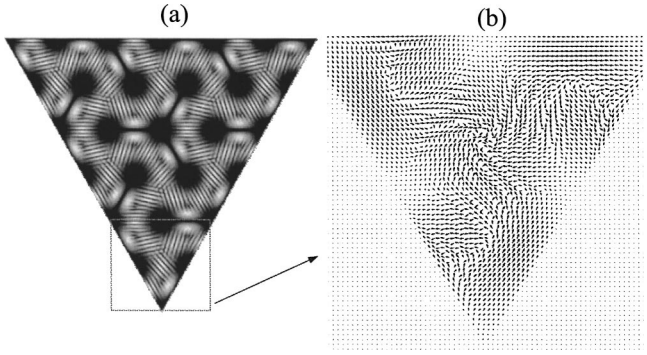

FIG. 4. (a) The wave pattern of the high-order coherent state $|\Psi_{N,M}(x,y;p,q,\phi)|^2$ from Eq. (6) with $p=q=3$, $\phi=\pi/2$, $N=10$, and $M=2p(N+1)$. (b) The corresponding quantum flux.

ity region. From nonseparable to chaotic billiards, quantum flux and vortex structures are expected to be further irregular, consistent with the random wave conjecture of Berry [22].

So far, for p and q to be relatively prime, the SU(2) coherent state corresponds to a single, nonrepeated orbit. Let l be the highest common factor of the indices p and q. If $l>1$, the coherent states are denoted to be high order. The wave patterns of high-order coherent states correspond to a combination of l primitive periodic orbits that are given by $(p/l,q/l,\phi_s/l)$, where $\phi_s=\phi+2\pi s$, $s\in\mathbb{Z}$, and $-l/2<s<(l/2-\phi/2\pi)$. In the case of $p=q$, the high-order coherent state displays a highly regular pattern. Hereafter we focus on the high-order coherent states with $p=q$. Numerical analyses reveal that for $\phi\neq 0$ or π the high-order coherent state typically exhibits an interlace pattern, as shown in Fig. 4(a) for $|\Psi_{N,M}(x,y;p,q,\phi)|^2$ with $p=q=3$, $\phi=\pi/2$, $N=10$, and $M=2p(N+1)$. Although the coherent state with $p=q=3$, $\phi=\pi/2$ is well localized on the three classical periodic orbits $(1,1,\pi/6)$, $(1,1,-3\pi/6)$, and $(1,1,5\pi/6)$, its intensity is like to be made up of woven threads which pass alternately over and under one another as they loop and knot around one another. As shown in Fig. 4(b), the corresponding flux vectors $\vec{J}$ are not straightaway but are swirling about the classical trajectories. Since the high-order coherent state has a regular periodic pattern, only a small region consisting of a unit trajectory is shown for fine details. It needs to be emphasized that the swirling, twisting quantum flux associated with the periodic orbits is fully induced by the confinement not by the magnetic field. Even so, weak perturbation plays a vital role for the appearance of the coherent states in mesoscopic quantum billiards [23].

In addition to the swirl vortex lattice, the high-order coherent states are found to form a triangular vortex lattice with phase synchronization $\phi=0$ and to form a *kagomè* vortex lattice with phase antisynchronization $\phi=\pi$, as show in Figs. 5(a) and 5(b) for $\Psi_{N,M}(x,y;p,q,\phi)$ with $p=q=6$, $N=10$, and $M=2p(N+1)$. The corresponding quantum flux vectors $\vec{J}$ for a unit trajectory are depicted in Figs. 5(c) and 5(d). It can be seen that the quantum flux vectors in the triangular and *kagomè* vortex lattices are relatively parallel to the classical velocity fields. Nevertheless, the main character, vortex-antivortex pair, is manifest in these vortex lattices.

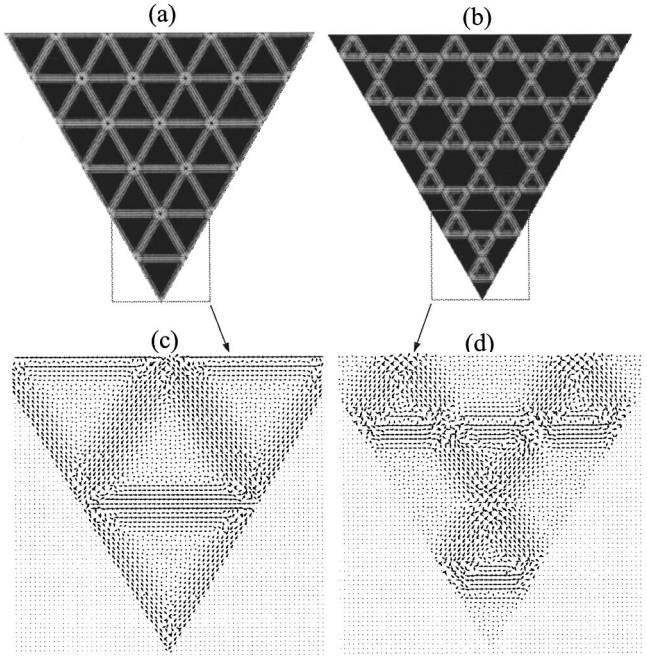

FIG. 5. The wave patterns for the high-order coherent states $|\Psi_{N,M}(x,y;p,q,\phi)|^2$ from Eq. (6) with $p=q=6$, $N=10$, and $M=2p(N+1)$: (a) $\phi=0$, a triangular vortex lattice; (b) $\phi=\pi$, a *kagomè* vortex lattice; (c) and (d) are the quantum flux vectors for (a) and (b), respectively.

Although vortex lattice states are well known in superconductor systems, their possibility in mesoscopic quantum billiards is likely to be ubiquitous [8,13]. More interestingly, the difference between the various vortex lattices only depend on the relative phase factor between various components of the coherent state.

In conclusion, the vortex formation associated with the classical periodic orbits in a nonseparable mesoscopic quantum billiard has been analytically studied. It is found that quantum interference effects lead to the well localization of the coherent state on the classical trajectories; however, the quantum probability flows may significantly differ from the classical velocity fields. On the other hand, the high-order coherent states are found to form the triangular, swirl, and *kagomè* vortex lattices. Theoretical results indicate that manipulating the phase factor of the high-order coherent state can lead to the transition between various vortex lattices. Since the phase factor of the coherent states is closely related to the initial position of the classical trajectories, from an experimental point of view, it can be changed by controlling the source of the excited wave. For instance, it has been demonstrated that controlling the excitation region in a large Fresnel number laser cavity can bring about various coherent patterns related to different phase factors [24,25].

ACKNOWLEDGMENT

The authors thank the National Science Council for their financial support of this research under Contract No. NSC-92-2112-M-009-013.

[1] L. F. Chibotaru, A. Ceulemans, V. Bruyndoncx, and V. V. Moshchalkov, Phys. Rev. Lett. **86**, 1323 (2001).
[2] B. J. Baelus and F. M. Peeters, Phys. Rev. B **65**, 104515 (2002).
[3] V. R. Misko, V. M. Fomin, J. T. Devreese, and V. V. Moshchalkov, Phys. Rev. Lett. **90**, 147003 (2003).
[4] E. L. Andronikashvili and Y. G. Mamaladze, Rev. Mod. Phys. **38**, 567 (1966).
[5] K. W. Madison, F. Chevy, W. Wohlleben, and J. Dalibard, Phys. Rev. Lett. **84**, 806 (2000).
[6] F. Dalfovo, S. Giorgini, L. P. Pitaevskii, and S. Stringari, Rev. Mod. Phys. **71**, 463 (1999).
[7] P. Dirac, Proc. R. Soc. London, Ser. A **133**, 60 (1931).
[8] Y. F. Chen, K. F. Huang, and Y. P. Lan, Phys. Rev. E **66**, 066210 (2002).
[9] S. Sridhar, Phys. Rev. Lett. **67**, 785 (1991).
[10] H. J. Stöckmann and J. Stein, Phys. Rev. Lett. **64**, 2215 (1990).
[11] Y. H. Kim, M. Barth, H. J. Stöckmann, and J. P. Bird, Phys. Rev. B **65**, 165317 (2002).
[12] K. F. Huang, Y. F. Chen, H. C. Lai, and Y. P. Lan, Phys. Rev. Lett. **89**, 224102 (2002).
[13] K. F. Berggren, A. F. Sadreev, and A. A. Starikov, Phys. Rev. E **66**, 016218 (2002).
[14] O. Olendski and L. Mikhailovska, Phys. Rev. E **67**, 056625 (2003).
[15] P. Šba, U. Kuhl, M. Barth, and H. J. Stöckmann, J. Phys. A **32**, 8225 (1999).
[16] P. Exner, P. Šeba, A. F. Sadreev, P. Středa, and P. Feher, Phys. Rev. Lett. **80**, 1710 (1998).
[17] L. Christensson, H. Linke, P. Omling, P. E. Lindelof, I. V. Zozoulenko, and K. F. Berggren, Phys. Rev. B **56**, 1440 (1997); J. P. Bird, R. Akis, D. K. Ferry, D. Vasileska, J. Cooper, Y. Aoyagi, and T. Sugano, Phys. Rev. Lett. **82**, 4691 (1999); R. Akis and D. K. Ferry, Phys. Rev. B **59**, 7529 (1999).
[18] M. A. Doncheski and R. W. Robinett, Ann. Phys. (N.Y.) **299**, 208 (2002).
[19] M. Brack and R. K. Badhuri, *Semiclassical Physics* (Addison-Wesley, Reading, MA, 1997).
[20] R. J. Richens and M. V. Berry, Physica D **2**, 495 (1981), G. B. Shaw, J. Phys. A **17**, 1537 (1974), W. K. Li and S. M. Blinder, J. Math. Phys. **26**, 2784 (1985).
[21] J. Pollet, O. Méplan, and C. Gignoux, J. Phys. A **28**, 7282 (1995).
[22] M. V. Berry, J. Phys. A **10**, 2083 (1977).
[23] R. Narevich, R. E. Prange, and O. Zaitsev, Phys. Rev. E **62**, 2046 (2000).
[24] Y. F. Chen and Y. P. Lan, Phys. Rev. A **66**, 053812 (2002).
[25] Y. F. Chen and Y. P. Lan, Phys. Rev. A **67**, 043814 (2003).